Energy Reports 8 (2022) 3323–3336

Contents lists available at ScienceDirect

Energy Reports

journal homepage: www.elsevier.com/locate/egyr

Research paper

Improved power quality operation of symmetrical and asymmetrical multilevel inverter using invasive weed optimization technique

Salman Ahmad [a], Atif Iqbal [b], Imtiaz Ashraf [c], Mohammad Meraj [b,*]

[a] Department of Electrical Engineering, Islamic University of Science and Technology, Awantipora, Pulwama, 192122, Jammu and Kashmir, India
[b] Department of Electrical Engineering, Qatar University, Doha, Qatar
[c] Department of Electrical Engineering, Aligarh Muslim University, Aligarh, India

ARTICLE INFO

Article history:
Received 10 October 2021
Received in revised form 29 December 2021
Accepted 16 January 2022
Available online 2 March 2022

Keywords:
Multilevel inverter
Low switching frequency
Invasive weed optimization
FPGA
Total harmonics distortion

ABSTRACT

Low switching frequency pulse width modulation (PWM) technique for modulation and control of multilevel inverter in medium voltage high power applications is preferred in order to reduce the switching losses. In this context, a multilevel inverter operated with Selective harmonics minimization PWM technique offers better quality waveform at reduced switching losses. After the Fourier series analysis, the system of non-linear simultaneous transcendental equations is obtained. These equations are then solved to obtain switching angles to have certain low order harmonics at minimum value and regulation in the fundamental voltage magnitude. In this paper, a novel invasive weed optimization (IWO) technique is proposed to compute switching angles. The proposed technique can compute switching angles for both symmetrical and asymmetrical multilevel inverters. Thus it has superiority over well-known optimization techniques such as GA, PSO, DE, and ACO, etc. Moreover, in certain modulation index ranges, it provides faster convergence and accurate results which have been demonstrated in the paper. The computational results have been verified with the experimental result on the prototype developed in the laboratory. The field programming gate arrays (FPGA) based controller is used to implement the proposed technique. The hardware results have been found in close agreement with the computed results.

1. Introduction

Voltage source inverters (VSI) are extensively used in many industrial applications such as active filters, variable speed drives, solar PV systems, wind energy, HVAC and HVDC transmission, electrical vehicles, etc. Earlier, only two-level and three-phase VSI configurations were mostly used (Levi et al., 2007; Chen and Zhao, 2016). But since the power processing requirements of power converters increased, the development of alternate topologies such as multilevel voltage source inverter with limited voltage and current ratings of the semiconductor devices has great attention in recent times (Wu and Narimani, 2017). The other advantages of multilevel inverters are low total harmonics distortion, low $\frac{dv}{dt}$ and low electromagnetic interferences(EMI). Various multilevel inverter topologies and its modulation and control schemes of multilevel inverters have been proposed in the literature (Colak et al., 2011; Gupta et al., 2015). The important topologies includes neutral point clamped (NPC), cascaded H-bridge (CHB), flying capacitor (FC), modular multilevel converter (MMC) and active neutral point clamped converters (ANPC) (Wu and Narimani, 2017). Several new topologies also have been proposed in recent year (Eguchi et al., 2020; Gupta et al., 2015). The promising topologies are Cascaded Half-Bridge based Multilevel DC Link (MLDCL) Inverter, T-type inverter, switched series/parallel sources (SSPS) based MLI, series connected switched sources (SCSS) based MLI, cascaded bipolar switched cells (CBSC) based MLI, multilevel module (MLM) based MLI, reversing voltage (RV) topology, two-switch enabled level-generation (2SELG) based MLI and packed E-cell topologies (Venkataramanaiah et al., 2017). These topologies are created while considering the low switching device counts, maximum possible number of levels, application oriented etc (Gupta and Bhatnagar, 2017). A detailed comparative analysis of popularly used multilevel inverter topologies is shown in Table 1. The number of devices are given for one leg of the inverter and 'n' represents the number of levels of the output phase voltage and 'V_{dc}' represents the dc-link voltage. In an NPC, more power diodes are used whereas, in an ANPC more number of active switches are used. Each topology have its own advantages and disadvantages and selection of any topology is application dependent (Kouro et al., 2010).

Power quality improvement in the output of voltage source inverter is desired for optimum performance in many applications

* Corresponding author.
E-mail addresses: salmanahmad19@gmail.com (S. Ahmad), mohammadmerajeee@gmail.com (M. Meraj).

https://doi.org/10.1016/j.egyr.2022.01.122

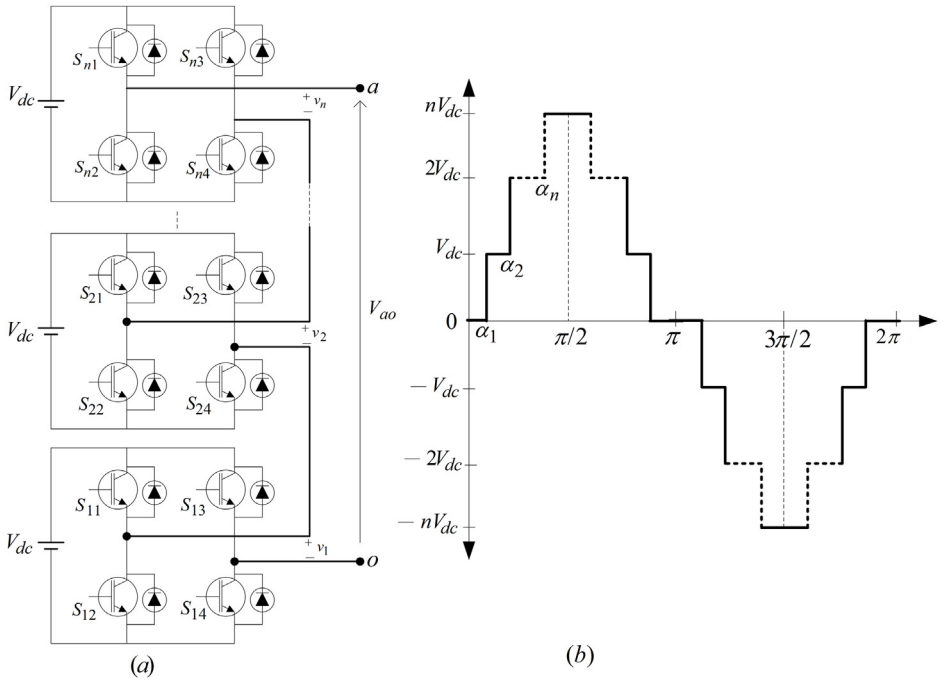

Fig. 1. One leg of a generalized cascaded H-bridge inverter.

Table 1
Comparative analysis of multilevel inverter topologies.

Parameters	NPC	FC	CHB	ANPC	MMC
Main switches	$2(n-1)$	$2(n-1)$	$2(n-1)$	$3(n-1)$	$2(n-1)$
Main diodes	$2(n-1)$	$2(n-1)$	$2(n-1)$	$3(n-1)$	$2(n-1)$
Clamping diodes	$(n-1)(n-2)$	–	–	–	–
DC-bus capacitor	$(n-1)$	$(n-1)$	$\frac{(n-1)}{2}$	–	–
Min. dc voltage	$2\sqrt{2}$	$2\sqrt{2}$	$2\sqrt{2}$	$2\sqrt{2}$	$2\sqrt{2}$
Voltage rating	$\frac{V_{dc}}{(n-1)}$	$\frac{V_{dc}}{(n-1)}$	$\frac{V_{dc}}{(n-1)}$	$\frac{V_{dc}}{(n-1)}$	$\frac{V_{dc}}{(n-1)}$
Component current	I	I	I	I	I
Cost	Medium	Medium	Medium	High	High

such as in solar photovolaic (Janardhan et al., 2020), shunt active filter (Chen et al., 2021), in SMPS and variable speed drives (Kularbphettong and Boonseng, 2020). The improved power quality operation of power converters have been proposed for applications such as in renewable power generation (Plangklang et al., 2016; Ahmed et al., 2021), dynamic voltage restorer (Bagdadee et al., 2020), variable speed drives (Kularbphettong and Boonseng, 2020), distributed power generation (Ali et al., 2021) etc. Pulse width Modulation (PWM) technique is widely used for the efficient operation of power electronics converters. It produces desired fundamental component and low undesired harmonic components. In literature, the high switching frequency based PWM techniques such as carrier based sine pulse width modulation (SPWM), space vector pulse width modulation (SVPWM) etc. have been extensively investigated and used (Holmes and Lipo, 2003). A high frequency carrier is continuously compared with a fundamental component (desired component) and at intersection points the pulses are generated in SPWM technique. Whereas, in space vector PWM the distinct switching states are first identified and the vectors are accordingly applied to obtain the desired output. The main advantage of high switching frequency (in kHz) techniques includes desired output fundamental component alongwith shifting of lower order harmonics at switching frequency as side band. Thus higher switching frequency will result in minimum filtering requirements. However, for medium voltage and high power applications, switching losses are the main constraints and therefore low switching frequency PWM techniques will be preferred (Edpuganti and Rathore, 2015; Tashakor et al., 2020). The selective harmonics elimination (SHE) PWM is one of the most promising modulation and control technique to obtain low switching losses and obtain a good quality waveform at the output (Dahidah et al., 2014). It is a pre-programmed PWM technique, which tries to optimize the harmonics profile while maintaining the desired fundamental component (Enjeti et al., 1988). The Fourier series analysis results in system of non-linear transcendental equations, which are simultaneously solved to obtain the switching angles that ensures removal of selected harmonics and control on fundamental component magnitude (Patel and Hoft, 1973). The system of non linear equations have multiple solutions, unique solution and non solution in certain range of modulation index (Chiasson et al., 2003). The best solution is normally chosen based on the minimum %THD, the difference in successive switching angles for practical implementation (Janabi et al., 2019), the next non eliminated harmonics magnitude (Kundu et al., 2019) and capacitor voltage balancing (Wu et al., 2020).

Several methods have been proposed in the literature to solve system of non-linear equations resulting from minimization of low order harmonics and control of fundamental component (Dahidah et al., 2014). These methods can be broadly classified as Numerical techniques based iterative methods (Ahmad et al., 2021), algebraic methods and meta-heuristic based optimization methods (Yang et al., 2015). The numerical techniques based methods includes Newton Raphson algorithm (N-R), Walsh function and sequential homotopy algorithm (Swift and Kamberis, 1993). The main advantage of numerical based techniques lies in the fact that they are fast convergent (quadratic in case of N-R) and their flexibility to be used for higher number of switching angles. However, these methods require an accurate initial guess very close to the actual switching angles (Salam et al., 2013). Also the solution trajectories in multilevel inverter is complex and not continuous in different range of modulation index, and the methods to choose initial guess in two level and three level inverter cases are not valid for multilevel case (Ahmed et al., 2019). Also as the number of switching angles increased (more number of levels), the numerical technique based methods

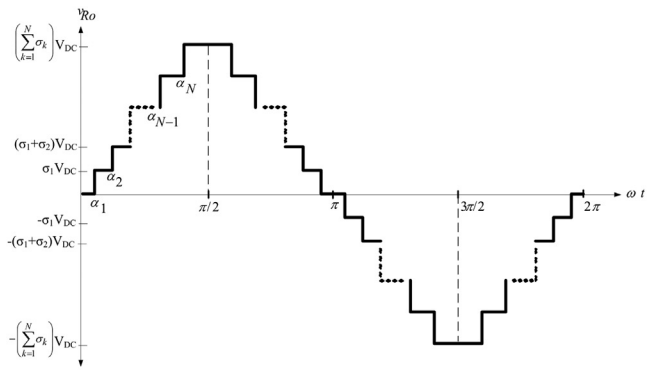

(a) (Fundamental switching

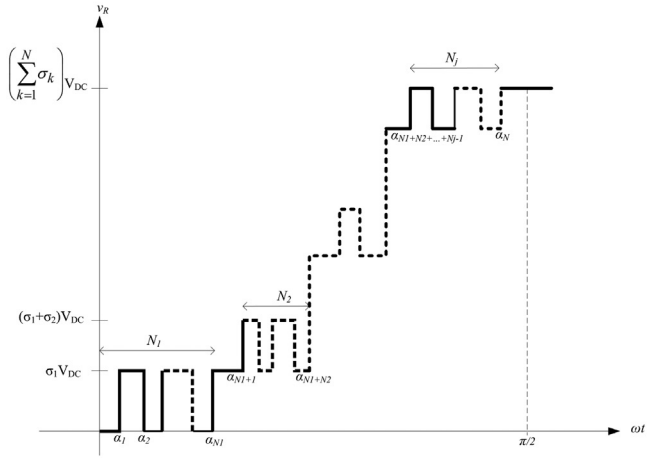

(b) Multiple switching

Fig. 2. Asymmetrical output waveforms.

suffers from the issue of singularity in the derivative matrix (Jacobian matrix) (Ahmad et al., 2019). The algebraic methods mainly includes theory of resultants, combination of symmetric polynomials and theory of resultant, parallel resultant, Wu method and Groebner bases method (Yang et al., 2015; Roberge et al., 2015). In algebraic methods the system of non linear SHE equations are first converted into polynomials by using multiple angles trigonometric formulas (e.g., $\cos(3\alpha) = 3\cos(\alpha) - 4\cos^3(\alpha)$ and so on) and then substituted with another variable for $\cos(\alpha)$ (say x). The new system of equations are solved and the switching angles are obtained by re-substituting ($\cos(\alpha) = x$). The algebraic methods provides exact and all the solutions of the problem and does not requires initial guesses. But for higher number of switching angles (more than four), the degree of polynomials also gets increased and solving it become very difficult. In literature the algebraic methods have been proposed to solve only for very few switching angles. The modern optimization techniques tried to solve for SHE equation are genetic algorithm (GA) (Kumari et al., 2019), particle swarm optimization (PSO) (Hagh et al., 2009; Panda and Panda, 2018), differential evolution (DE) (Salam et al., 2015), ant colony optimization (ACO) (Sundareswaran et al., 2007), Colonial competitive algorithm (CCA) (Etesami et al., 2015), artificial bee colony optimization (ABC) (Kavousi et al., 2011), teaching–learning (TL) based optimization technique (Haghdar, 2019), FPA based technique (Panda et al., 2020) and several hybrid techniques such as bio inspired intelligent algorithms (Memon et al., 2018), Particle swarm-genetic algorithm (Memon et al., 2021), and differential search algorithm (DSA) (Kundu et al., 2017).

Although the optimization based techniques proposed in literature successfully solve the harmonics minimization problem, but still there are certain limitations on these methods. For instance, the limitations for GA includes a premature convergence and weakness in local search capability in addition to slow convergence rate. The PSO do not have cross over and mutation operators and therefore has fast convergence but it requires a very fine tuning in the search space. Therefore, as the number of switching angles are increased, the complexity of tuning in search space gets increased as well and it trapped in local optimal solutions. In this paper a novel invasive weed optimization (IWO) meta-heuristic technique is proposed to solve for the harmonics minimization equations. The harmonics minimization problem of both symmetrical and asymmetrical multilevel inverter configurations can be solved by this method. Some improved IWO version are also proposed to solve for the harmonics minimization equations and the performance are compared with the existing methods in the literature. The convergence rate and accuracy of the results found better in comparison to the other optimization techniques. Moreover, the proposed method is capable in computing switching angles for any inverter topologies discussed above and for multiple switching of individual cells. Rest of the paper is organized as follows: In Section 2, mathematical modelling of CHB for symmetrical and asymmetrical configuration with harmonics minimization equations problem formulation is given, in Section 3, IWO methods and its implementation in solving system of non-linear equations is given. In Section 4 computational results and comparative analysis with other methods is given, in Section 5 experimental set-up and hardware results is given and finally in Section 6, conclusion of the work is given.

2. Problem formulation

In CHB, several H-cells are connected in series to obtain multi level output waveform. If there are n separate DC sources then $2n + 1$ level output waveform is obtained. A generalized single phase symmetrical CHB configuration with n number of separate DC sources and corresponding multilevel waveform is shown in Fig. 1(a) and Fig. 1(b) respectively. After the Fourier series analysis of waveform in Fig. 1(b), the output voltage is given by (1).

$$V_{ao} = b_h \left[\sum_{h=1}^{\infty} \sin(h\omega t)\right] \tag{1}$$

Where, b_h is the peak magnitude of hth harmonics ($h = 1$, fundamental component). Since the output waveform is having both the half wave and quarter wave symmetries, the expression for b_h after simplification will result in (2).

$$b_h = \begin{cases} \frac{4V_{dc}}{h\pi}\left[\sum_{k=1}^{n}\cos(h\alpha_k)\right] & , for\ odd\ h \\ 0 & , for\ even\ h \end{cases} \tag{2}$$

For 11-level, three-phase cascaded H-bridge multilevel inverter (five switching angles in a quarter period), the harmonics minimization equations for quarter wave symmetric waveform considering the elimination of low order non triplen harmonics such as 5th, 7th, 11th and 13th from the final output waveform and control over fundamental components is given by (3). If the non equality coefficients,

$$\begin{cases} \frac{4V_{DC}}{\pi}\left[\cos(\alpha_1)+\cos(\alpha_2)+\cos(\alpha_3)+\cos(\alpha_4)+\cos(\alpha_5)\right] - 5\times M \le \epsilon_1 \\ \cos(5\alpha_1)+\cos(5\alpha_2)+\cos(5\alpha_3)+\cos(5\alpha_4)+\cos(5\alpha_5) \le \epsilon_2 \\ \cos(7\alpha_1)+\cos(7\alpha_2)+\cos(7\alpha_3)+\cos(7\alpha_4)+\cos(7\alpha_5) \le \epsilon_3 \\ \cos(11\alpha_1)+\cos(11\alpha_2)+\cos(11\alpha_3)+\cos(11\alpha_4)+\cos(11\alpha_5) \le \epsilon_4 \\ \cos(13\alpha_1)+\cos(13\alpha_2)+\cos(13\alpha_3)+\cos(13\alpha_4)+\cos(13\alpha_5) \le \epsilon_5 \\ Where,\ M = \frac{\pi}{4}\frac{V_1}{V_{dc}}\ and\ , 0 \le M \le 1; \\ 0 \le \alpha_1 \le \alpha_2 \le \alpha_3 \cdots \le \alpha_N \le \frac{\pi}{2} \end{cases} \tag{3}$$

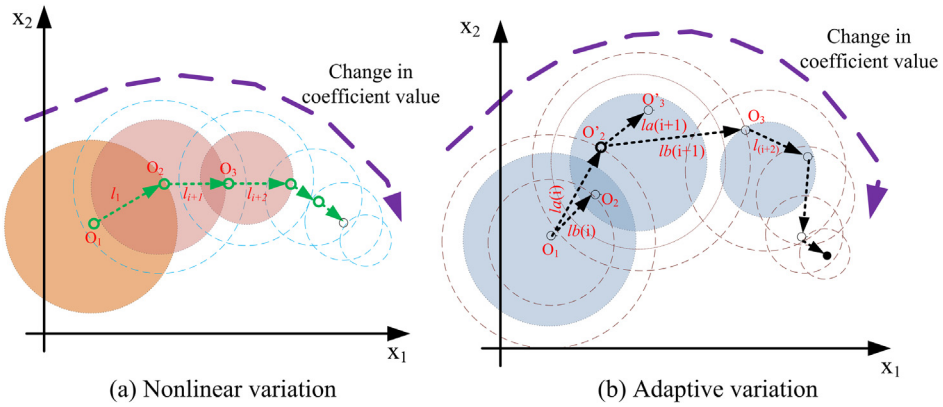

Fig. 3. Seed movements between iterations.

ϵ_1, ϵ_2, ϵ_3, ϵ_4, ϵ_5 are considered to be zero, the harmonics minimization problem will transformed into selective harmonics elimination problem. Let, the non equal separate DC sources are considered as $V_{DC1} = \sigma_1 V_{DC}$, $V_{DC2} = \sigma_2 V_{DC}$, $\cdots$, $V_{DCn} = \sigma_n V_{DC}$, where $\sigma_1, \sigma_2, \ldots, \sigma_n$. The corresponding, asymmetrical waveforms for fundamental switching and multiple of switching is shown in Fig. 2(a) and Fig. 2(b) respectively. In Fig. 2(b), $N_1, N_2, \ldots, N_i$ represents the number of switching of cell '1', cell '2'...cell 'i' respectively. The generalized expression to eliminate non triplen harmonics in three phase multilevel inverter having balanced load for multiple switching with non equal dc sources can be given by (4). Here, L represents the number of levels in the output waveform and 'N' represents the total of switching of all the cell in one time period.

3. Invasive weed optimization

Invasive weed optimization (iwo) technique was first developed by Mehrabian and Lucas in 2006 (Mehrabian and Lucas, 2006). The iwo is a population based meta-heuristic algorithm based on the concept of ecological system that mimics the behavioural and survival properties of the weeds to grow, reproduce and colonize the whole area. The individual weeds in the iwo algorithm is a potential solution of the problem and encoded as row vector with multiple variables. The main steps in iwo algorithm includes population initialization, spacial dispersal, reproduction of offspring's

$$\frac{4V_{DC}}{\pi}\left(\sigma_1\sum_{i=1}^{N_1}(-1)^{i-1}\cos(\alpha_i)+\sigma_2\sum_{i=N_1+1}^{N_1+N_2}(-1)^{i}\cos(\alpha_i)+\cdots+\sigma_k\sum_{i=N_1+N_2+\cdots}^{N}(-1)^{i+1}\cos(\alpha_i)\right)-\frac{L-1}{2}\times M\le\epsilon_1$$

$$\sigma_1\sum_{i=1}^{N_1}(-1)^{i-1}\cos(5\alpha_i)+\sigma_2\sum_{i=N_1+1}^{N_1+N_2}(-1)^{i}\cos(5\alpha_i)+\cdots+\sigma_k\sum_{i=N_1+N_2+\cdots}^{N}(-1)^{i+1}\cos(5\alpha_i)\le\epsilon_2$$

$$\vdots$$

$$\sigma_1\sum_{i=1}^{N_1}(-1)^{i-1}\cos(n\alpha_i)+\sigma_2\sum_{i=N_1+1}^{N_1+N_2}(-1)^{i}\cos(n\alpha_i)+\cdots+\sigma_k\sum_{i=N_1+N_2+\cdots}^{N}(-1)^{i+1}\cos(n\alpha_i)\le\epsilon_n$$

Where, $n = 5, 7, 11\cdots$ *and*

$$0\le\alpha_1\le\alpha_2\le\cdots\alpha_{N_1}\le\alpha_{N_1+1}\le\cdots\le\alpha_N\le\frac{\pi}{2} \tag{4}$$

and competitive selection or rejection. The initial population of invasive weed plants are randomly spread in the search space and reproduces off-spring seeds within the search space. The initial random population is generated using (5).

$$\alpha_i = \left(\alpha_i^{max}-\alpha_i^{min}\right)\times rand(0,1)+\alpha_i^{min} \tag{5}$$

Where, α_i^{max} is $\pi/2$ and α_i^{min} is 0 for quarter wave symmetrical output waveform shown in Fig. 2. After initialization each weed (parent weed) reproduces new offspring's seeds depending upon the relative fitness i.e. the best member weed will produce more number of offspring's than the worst member weeds. These newly reproduced are randomly scattered around the parents weed in the next step. This spatial dispersions are according to the normal distribution around the parent weeds (Misaghi and Yaghoobi, 2019). The number of offspring's reproduced from the *k*th parent is calculated using (6).

$$N_{seed,k} = \frac{F_{fitness,k}-F_{min,j}}{F_{max,j}-F_{min,j}}\times\left(N_{S,max}-N_{S,min}\right)+N_{S,min} \tag{6}$$

Where, $N_{seed,k}$ is number of seeds from the *k*th parent and $F_{fitness,k}$, $F_{min,j}$, $F_{max,j}$ are the fitness values of *k*th parent weed, minimum and maximum fitness values of the parents in the current iteration respectively. $N_{S,min}$ and $N_{S,max}$ are the minimum and maximum number of offspring seeds produced by *k*th parent.

3.1. Exponential seed spread IWO

The modifications in originally proposed IWO algorithm is made to achieve more robust optimization so that there is a balance in local and global optimization searches. Moreover, accurate results and faster convergence should also be achieved. The exponential standard deviation (SD) in the spreading factor is introduced for this purpose. Therefore, the new SD is defined as in (7).

$$\gamma_{iter,SD} = \left(e^{\left[\tau\left[\frac{iter_i}{iter_{max}}\right]^m\right]}\right)(\gamma_{initial}-\gamma_{final})+\gamma_{final} \tag{7}$$

Where, $\gamma_{initial}$, γ_{final} and $iter_{max}$ are describing parameter setting for SD, whereas m and τ describes the shape of the exponential slope of SD during the iterations. The rate of seed spreading evolution factor (SSF) is introduced for faster convergence of the algorithm towards global optimum. The SSF utilize the previous iterations local knowledge to obtain improved standard deviation.

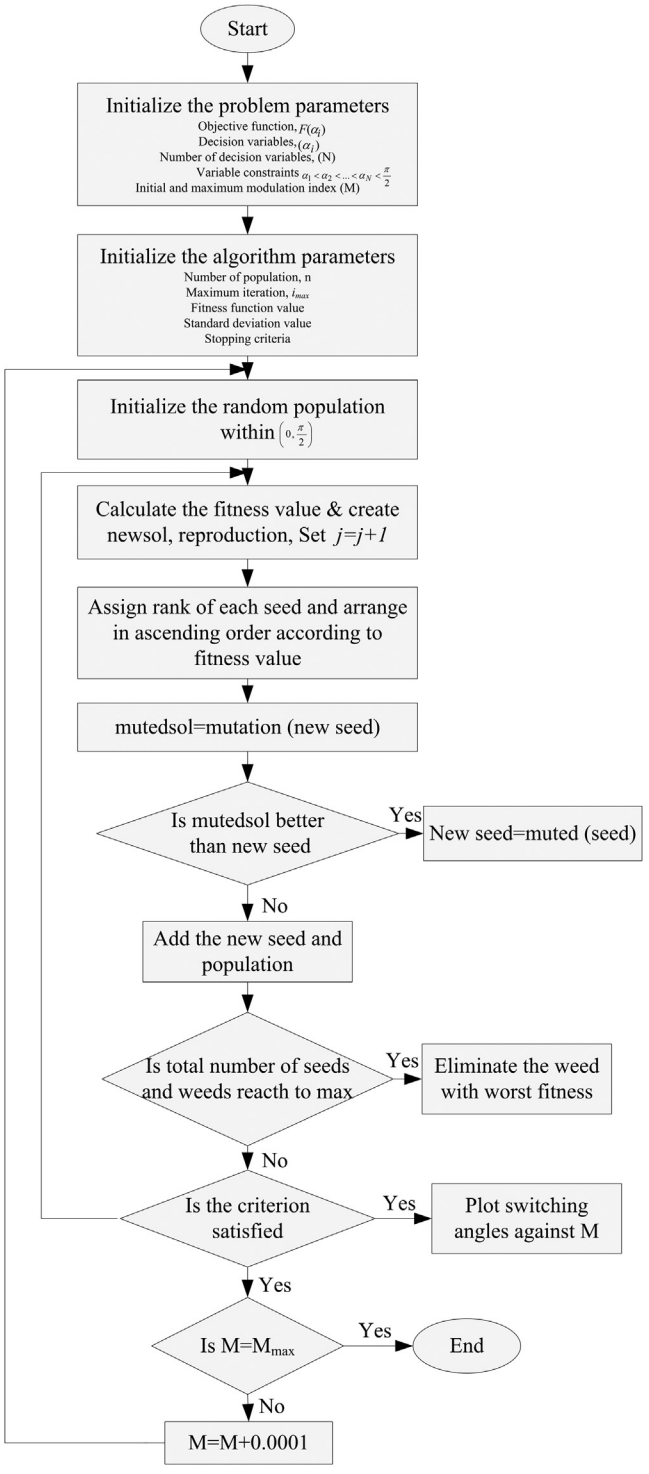

Fig. 4. IWO algorithm to compute switching angles.

The SSF is mathematically represented by (8).

$$C = \left[\frac{|F_i| - F_{worst}}{F_{best} - F_{worst}}\right](C_i' - C_f') + C_f' \tag{8}$$

Where, C is the normalized SF, F_i is fitness function value of current weed, F_{best} and F_{worst} are the best and worst fitness function values up to that iteration, C_i' and C_f' are the SSF factors initial and final values. The rate of SSF is changes accordingly in the subsequent iterations. Normally the value of normalized spread factor lies in $0 \leq C \leq 1$. The magnitude of 'C' reflects the seeds spreading capability and smaller value means faster the speed. Therefore, the spreading factor is modified as in (9).

$$\gamma_{iter,SD_{eSSF}} = C \times \left(e^{\left[\tau\left[\frac{iter_i}{iter_{max}}\right]^m\right]}\right)(\gamma_{initial} - \gamma_{final}) + \gamma_{final} \tag{9}$$

Here, $\gamma_{iter,SD_{eSSF}}$ is the new SD and C is the SSF value given in (8). With increase in number of iterations, SD decreases exponentially. If current best and global best differ by large margin, the factor C will be high and will result large value of SD and vice-versa. Another modification to expedite, the seed spread mechanism is proposed by modifying the value of C in (10) in order to control the changes in SD.

$$C_{new} = \frac{1}{e^{\left[\frac{|F_i| - F_{worst}}{F_{best} - F_{worst}}\right]}}(C_i' - C_f') + C_f' \tag{10}$$

Therefore, in modified invasive weed optimization (MIWO) based on the exponential seed spread factor (eSSF), the SD is finally given by (11).

$$\gamma_{iter_{MIWO}} = C_{new} \times \left(e^{\left[\tau\left[\frac{iter_i}{iter_{max}}\right]^m\right]}\right)(\gamma_{initial} - \gamma_{final}) + \gamma_{final} \tag{11}$$

The modified expression in (11), ensures better exploration ability of the seeds in the vicinity of current best and thus will converges towards optimum values. The optimum search of weeds in invasive weed optimization and exponential weed optimization (eIWO) with exponential weed spreading is illustrated in Fig. 3. The radius of the round shapes decreases non-linearly during iterations in the search operations, where radius l, of the round shapes depicts the standard deviation. However, in (eIWO), the standard deviation either vary as l_{ai} or l_{bi}, further it will vary either $l_{a(i+1)}$ or $l_{b(i+1)}$ as illustrated in Fig. 3(b) . The magnitude of standard deviation in this case will depend on C for IWO variation using eSSF or C_{new} for MIWO based eSSF given in (8) and (10) respectively.

3.2. IWO algorithm

To compute the wider range of solution from the highly non linear sets of transcendental equations is important. In this context the meta heuristic based optimization techniques provides the requisite solutions. Although these methods do not provide exact solutions, but by having proper adjustment in objective function and the way algorithm is implemented we can ensure to maintain a minimum magnitude of the certain harmonics to be minimized. The low switching frequency operation of VSI is also ensured by having minimum THD while keeping certain lower order harmonics at a minimum level. This can be achieved by incorporating it in the objective function. In this chapter a detailed analysis of various optimization techniques in solving the various cases of sets of non linear transcendental equations have been carried out. The optimization problem in several variables with certain constraints in generic from is expressed by (12).

$$\begin{array}{lll} \text{Minimize} & f(\boldsymbol{\alpha}) & \\ \text{Subject to} & g_u(\boldsymbol{\alpha}) \leq 0; & u = 1, \ldots, p \\ & h_v(\boldsymbol{\alpha}) = 0; & v = 1, \ldots, q \\ & \alpha_w \geq 0; & w = 1, \ldots, r \end{array} \tag{12}$$

Where, $g_u(\boldsymbol{\alpha})$ and $h_v(\boldsymbol{\alpha})$ are functions of design vectors $\alpha = (\alpha_1, \alpha_2, \ldots, \alpha_d)^T$ and $f(\boldsymbol{\alpha})$ is called objective function or cost function to be minimized. To incorporate constraints in the optimization process, there are many ways such as penalty method, transformation method, separation of objective and constraints, stochastic ranking methods etc. In this work, penalty method is considered for handling the constraints on the switching angles.

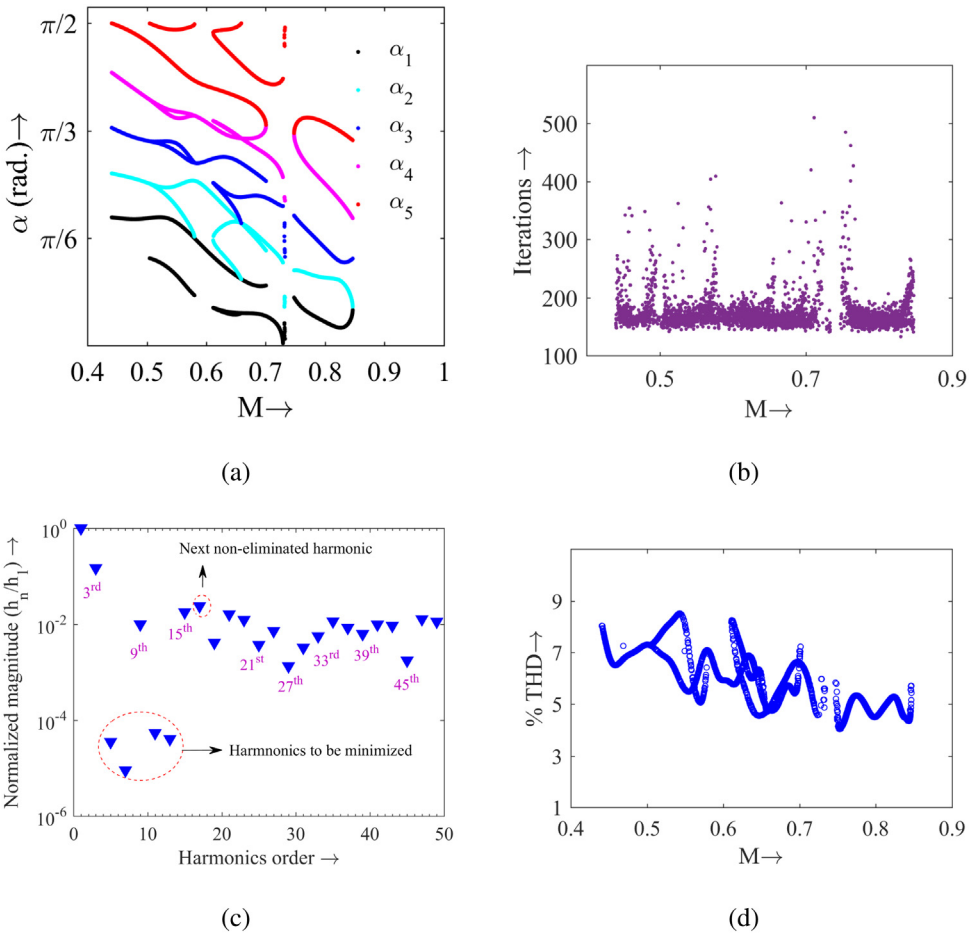

Fig. 5. Computational results for 11-level symmetrical output.

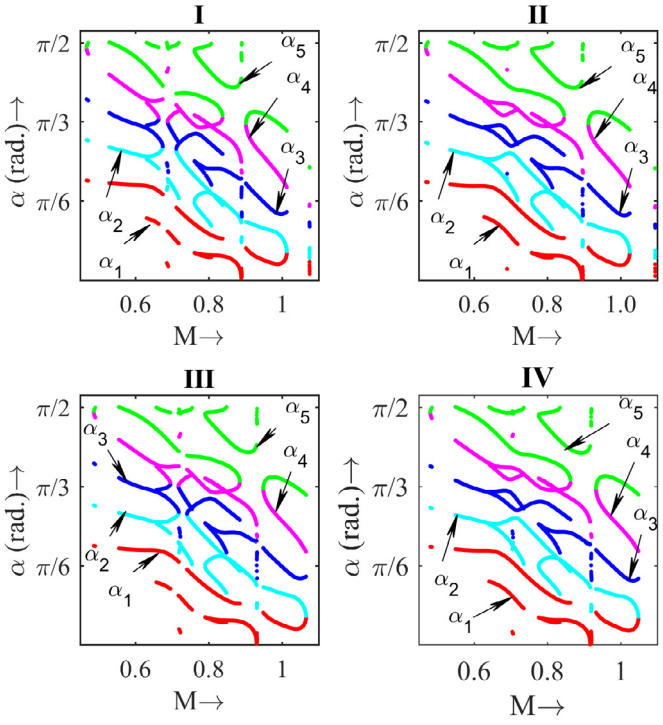

Fig. 6. Switching angle trajectories for 11-level asymmetrical cases.

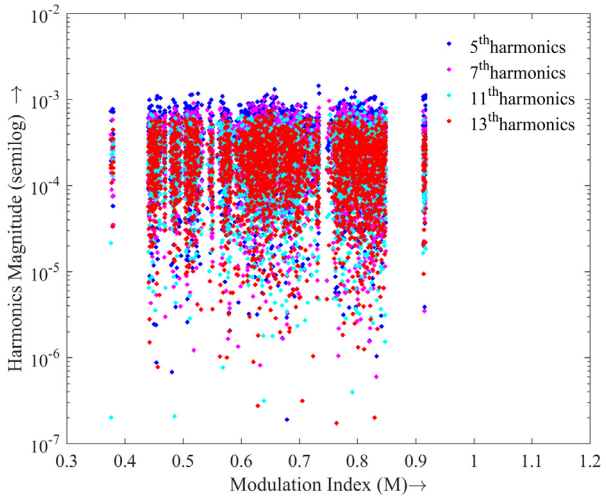

Fig. 7. Magnitude of 5th, 7th, 11th and 13th order harmonics.

The penalty method tries to convert a constrained optimization problem into an unconstrained problem by incorporating defined constrains into objective function and thus a new objective function is defined which is optimized using various optimization techniques. The problem defined in (12) can be converted into an equivalent unstrained optimization problem by using new

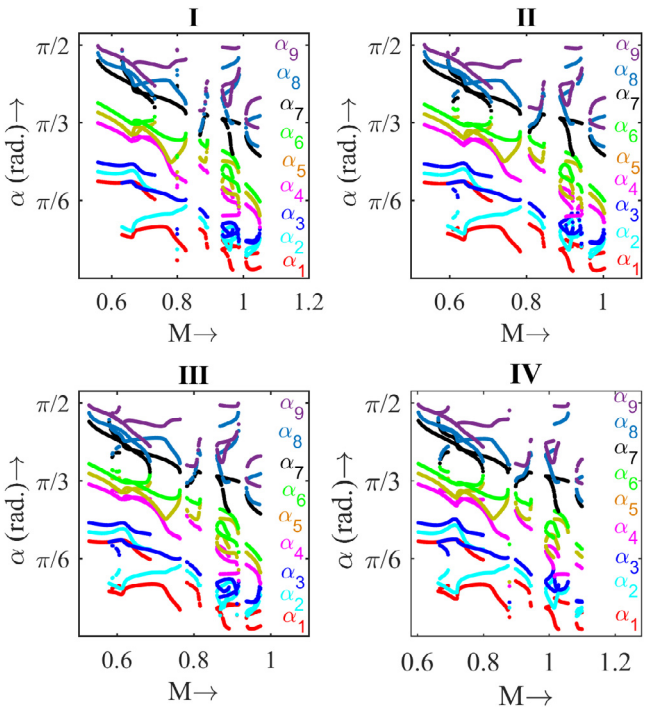

Fig. 8. Asymmetrical seven level multiple switching trajectories.

Table 2
Main parameter values of IWO.

Parameters	Values
Initial population size (n_{pop_0})	10
Maximum population size (n_{pop})	25
Minimum number of seeds (S_{min})	0
Maximum number of seeds (S_{max})	5
Variance reduction exponent	2
Initial value of standard deviation ($\sigma_{initial}$)	0.25
Final value of standard deviation (σ_{final})	0.001

objective function defined in (13).

Minimize

$$F(\boldsymbol{\alpha}) = f(\boldsymbol{\alpha}) + \sum_{u=1}^{p} r_u \langle g_u(\boldsymbol{\alpha})\rangle^2 + \sum_{v=1}^{q} R_v \left(h_v(\boldsymbol{\alpha})\right)^2 \tag{13}$$

Where, r_u and R_v are the penalty parameters linked with constraints $g_u(\boldsymbol{\alpha})$ and $h_v(\boldsymbol{\alpha})$ respectively and have a fixed value throughout the optimization process. in (13), $\langle g_u(\boldsymbol{\alpha})\rangle$, called the bracket function and is defined as given in (14).

$$\langle g_u(\boldsymbol{\alpha})\rangle = \begin{cases} g_u(\boldsymbol{\alpha}), & \text{if } g_u(\boldsymbol{\alpha}) > 0 \\ 0, & \text{if } g_u(\boldsymbol{\alpha}) < 0 \end{cases} \tag{14}$$

The optimization problem is formulated by first having an objective function which is to be minimized (Rao, 2019). Here objective function is constructed by considering lower order harmonics components to be minimum while controlling the fundamental component magnitude. The primary objective in formulating an objective function is to achieve the desired fundamental voltage component. The next priority is to suppress the lower order harmonics components as per their rank (lowest order have more priority).

$$F = \min_{\alpha_k} \left\{ \left(100 \times \frac{V_1^* - V_1}{V_1^*}\right)^4 + \sum_{k=2}^{N} \frac{1}{h_k} \left(50 \times \frac{V_{h_k}}{V_1}\right)^2 \right\} \tag{15}$$

$$0 \le \alpha_1 \le \alpha_2 \le \cdots \alpha_{N-1} \le \alpha_N \le \frac{\pi}{2} \tag{16}$$

Table 3
Switching angles of $3-\phi$, 11 level CHB inverter (Deg.).

$M \rightarrow$	0.378	0.453	0.504	0.600	0.650	0.700	0.750	0.800	0.917
α_1	35.80	34.49	23.65	25.91	18.89	16.21	11.98	6.36	4.42
α_2	49.43	46.17	43.84	42.68	34.50	25.81	20.40	18.37	7.77
α_3	64.83	57.97	55.31	49.93	50.16	44.56	34.41	26.31	19.44
α_4	83.26	72.43	66.62	60.57	56.29	58.94	54.00	43.74	24.88
α_5	87.22	86.46	87.27	70.33	67.50	60.32	60.08	60.34	40.31
THD	**10.6%**	**8.5%**	**8.1%**	**6.9%**	**6.5%**	**6.4%**	**5.4%**	**5.3%**	**4.5%**

Table 4
Asymmetrical cases for 11-level Inverter.

Case	Unbalancing factors
I	$\sigma_1 = 1.08, \sigma_2 = 0.98, \sigma_3 = 0.90, \sigma_4 = 0.86, \sigma_5 = 0.80$
II	$\sigma_1 = 1.02, \sigma_2 = 0.99, \sigma_3 = 0.95, \sigma_4 = 0.89, \sigma_5 = 0.85$
III	$\sigma_1 = 1.10, \sigma_2 = 1.05, \sigma_3 = 0.95, \sigma_4 = 0.90, \sigma_5 = 0.88$
IV	$\sigma_1 = 1.04, \sigma_2 = 1.01, \sigma_3 = 0.98, \sigma_4 = 0.92, \sigma_5 = 0.85$

In (15), V_1^* is the required fundamental component and h_k kth harmonics magnitude. The 4th degree penalty is applied for any violation in desired fundamental component by more than 1%. The harmonics magnitude considered for minimization, the penalty function of degree 2 is considered, whenever its relative magnitude with fundamental component deviated by more than 2%. The factor h_k provides more weight in minimization of lower order harmonics component. The objective function and constraint thus formulated are solved using IWO algorithm. The flow chart for obtaining switching angles for minimum magnitude of selected harmonics and to have control on fundamental component for various cases of multilevel inverter as function of modulation index (M) is shown in Fig. 4. The flowchart for multiple switching cases can be implemented in the similar fashion with incorporation of number of switching of individual H cells in the algorithm. The main algorithm parameters are given in Table 2.

4. Computational results

The computational results for symmetrical and asymmetrical configurations of multilevel inverter using the IWO technique are given in this section. The fundamental switching frequency and multiple of fundamental switching frequency cases have been considered to demonstrate the effectiveness of the proposed technique. Harmonics up to order of 49th, i.e. 2450 Hz have been considered in the formulation of objective function. The selected non triplen low order harmonics have been taken for minimization along-with control of the fundamental component (expressed in terms of modulation index). Since quarter wave symmetric waveform has been taken, the switching angles must satisfy the constraints illustrated in (16). The trajectory of switching angles for 11-level waveform are shown in Fig. 5(a), iterations as function of modulation index in Fig. 5(b), harmonics profile in Fig. 5(c) and %THD in Fig. 5(d) respectively. The targeted harmonics for minimization from the output waveform have very small value as confirmed from the harmonics profile. The switching angles trajectories for asymmetrical cases given in Table 4 have been shown in Fig. 6. The trajectories clearly depicts different number of solutions in different range of modulation index. The switching angles in degree as function of modulation index and *%THD* as function of modulation index for 11-level symmetrical CHB for fundamental switching frequency have been shown in Table 3. The magnitude of harmonics considered for minimization i.e 5th, 7th, 11th and 13th have been shown in Fig. 7.

The switching angle trajectories for seven level waveform with three times the fundamental switching frequency are shown

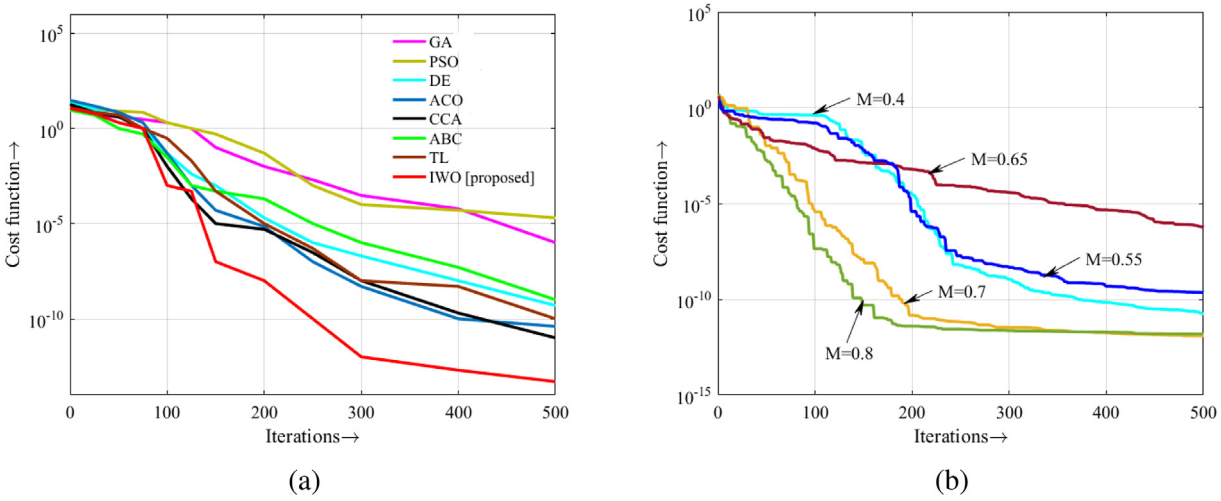

Fig. 9. (a) Comparison of various algorithm (b) Comparison of cost function at various modulation index by IWO.

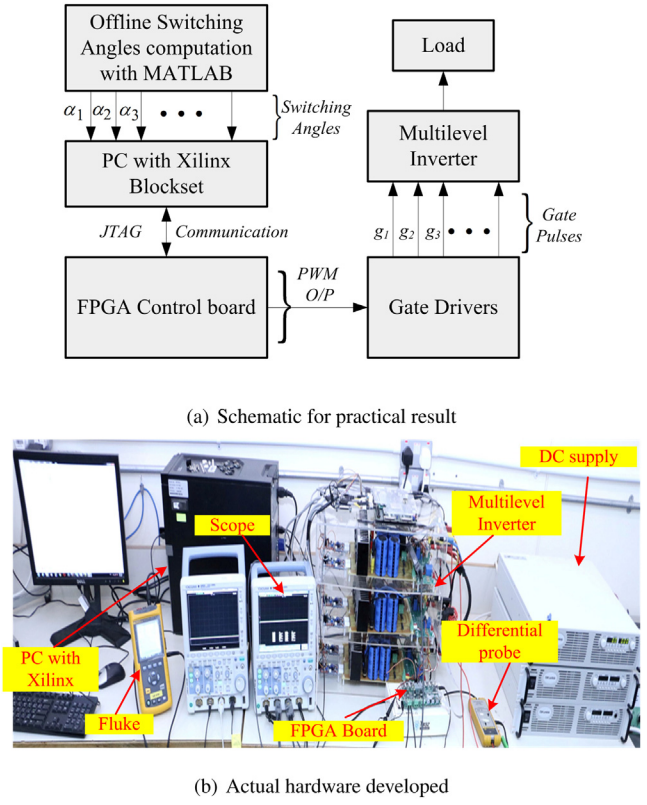

(a) Schematic for practical result

(b) Actual hardware developed

Fig. 10. Hardware setup for experimental results.

in Fig. 8. The dc voltages are taken in the ratio given in Table 5. The targeted harmonics for minimization are considered to be 5th, 7th, 11th, 13th, 17th, 19th, 23rd and 25th. In multiple switching cases as well, there are unique solution, multiple solution and no solution in different range of modulation index. More number of harmonics can be eliminated with higher number of switching of individual H cell, but the switching losses will also increase. So there is a trade-off between switching losses and output power quality.

The comparative analysis of various algorithm in terms of cost function vs number if iteration is shown in Fig. 9(a). The minimization problem for 11-level symmetrical output at fundamental switching frequency has been considered with same

Table 5
Multiple switching 7-level non-equality cases.

Case	Unbalancing factors
I	$\sigma_1 = 1.1, \sigma_2 = 0.97, \sigma_3 = 0.92$
II	$\sigma_1 = 1.02, \sigma_2 = 0.95, \sigma_3 = 0.90$
III	$\sigma_1 = 0.98, \sigma_2 = 0.94, \sigma_3 = 0.85$
IV	$\sigma_1 = 1.12, \sigma_2 = 1.08, \sigma_3 = 1.02$

objective function. Also, the cost function values at different modulation index as function of iteration is shown in Fig. 9(b). Form Fig. 9(a), it can be observed that the IWO algorithm performs better and therefore it requires lesser computational time due to fast convergence. In this study, the change in modulation index is very small (0.0001), despite of the fact that at some at point the solution does not converges, still we get enough solution to obtain the desired solution trajectories as function of M. It is also producing all possible solutions for fundamental switching frequency and multiple of fundamental switching frequency. Moreover, the proposed IWO algorithm is capable in producing all possible results for any inverter topology. The steps involved in solving are also very less in comparison to the other optimization techniques proposed in the past for solving harmonics minimization problem. The real time implementation of the switching angles computed off-line can be achieved by the methods proposed in the literatures. The main methods include artificial neural network (ANN) (Tolbert et al., 2011), adaptive artificial neural network (Maia et al., 2012) and Hopfield neural network (HNN) (Balasubramonian and Rajamani, 2014). In these methods a network is trained from the computed input and output dataset. The trained network is then utilized for real time implementation.

5. Experimental results

The prototype is developed in the laboratory to test the computational results discussed in the previous section. The schematic and actual hardware are shown in Fig. 10(a) and Fig. 10(b) respectively. The H-bridge controlled switches are bidirectional IGBT selected from Semikron SKM100GB12T4. The control logic have been developed and switching angles have been tested using field programmable gate arrays (FPGA) VIRTEX- 5 XC5VLX50T based digital controller. The oscilloscope and spectrum analyzer have been used to record the output waveforms and harmonics spectrum respectively. The gate control signal from FPGA is given

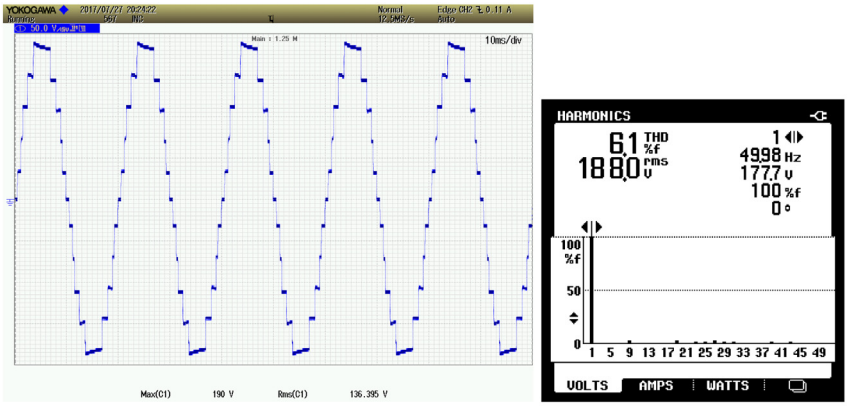

(a) Output voltage (b) Harmonics profile

(c) Output voltage (d) Harmonics profile

Fig. 11. 11-level output voltage and harmonics profile.

Table 6
Prototype components and rating.

Components	Ratings
SIC-MOSFET ($S_{T1} - S_{T4}$)	FDP19N40 (1200V, 40A)
DC Power supply	TDK-Lambda GEN (0-100V, 15 A)
Digital Controller	Virtex-5 FPGA
Switching frequency (f_{sw})	50–150 Hz
Load	1.0 kW

to IGBT gate drivers which in turn provides adequate signal to the switches for proper turn on and turn off. The FPGA board used in the experiment offers a 50 MHz clock frequency and therefore a time resolution of 20 nanoseconds of gate signal is achieved. Since two switches never turned ON simultaneously in the same leg, the dead time is not required and thus it eases the control implementation. Moreover, The high time resolution and absence of dead time requirements eliminates the possibility of pulse dropping if the difference in consecutive switching angles is very small. The components rating of prototype is given in Table 6.

5.0.1. Symmetrical stepped waveform

The reference sine signal is compared with a constant line having magnitude equal to the sine of computed switching angles. The 11-level waveform with corresponding harmonics profile is shown in Fig. 11. The switching frequency in this experiment is kept at fundamental frequency i.e., 50 Hz. The targeted harmonics for minimization such as 5th, 7th, 11th and 13th are absent in the harmonics profile.

5.0.2. Asymmetrical stepped waveform

The programmed DC supply tdk lambda with voltage range of $0-100V$ in a fine step of $0.1V$ is used for each H-bridge. Unequal voltages in each H cell is easily obtained to verify the computation results discussed in the previous section. The computed switching angles for 11-level asymmetrical H-bridge inverter have been implemented by comparing with a reference sine signal in FPGA control board. The output voltage waveform and harmonics profiles for $M = 0.55$ and $M = 0.62$ are shown in Fig. 12. The hardware result clearly indicates that the targeted harmonics are minimum.

The dynamic behaviour of the proposed algorithm has been shown in Fig. 13 by step change in the load. The no load condition is first considered, 50% load and then full load. In the experiment, an RL load is taken and figure shows the increase in load current with increase in the load magnitude. Similarly the dynamic behaviour of the proposed algorithm can obtained by increasing the load. The sine PWM waveform for the same inverter at 10 kHZ switching frequency is shown in Fig. 14 with change in load from no load to 50% load to full load. The load current is more smooth, but the switching losses will be more and will be significant in medium voltage high power application of power converters.

5.0.3. Multiple pulsed multilevel waveform

In multiple switching the individual cells are turned ON and OFF more than once in a quarter period. The FPGA control signal is implemented by generating reference sine wave and it is compared with the sine value of computed switching angles. If seven level inverter with three times the fundamental frequency

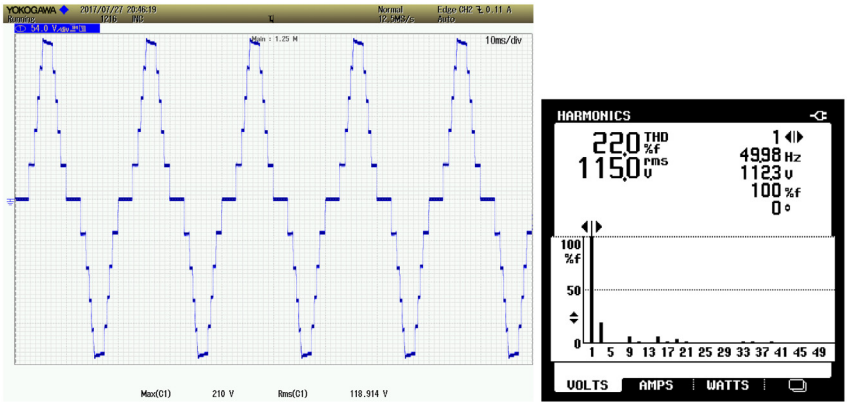

(a) Output voltage (b) Harmonics, M=0.55

(c) Output voltage (d) Harmonics, M=0.62

Fig. 12. 11-level asymmetrical waveform and harmonics profile.

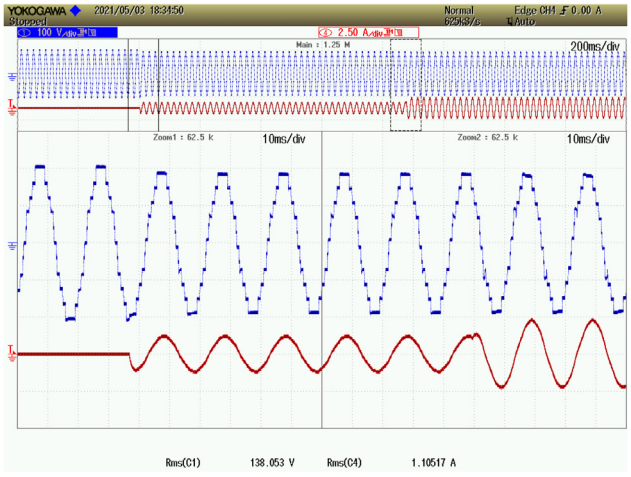

Fig. 13. Dynamic behaviour of the algorithm on step change in load.

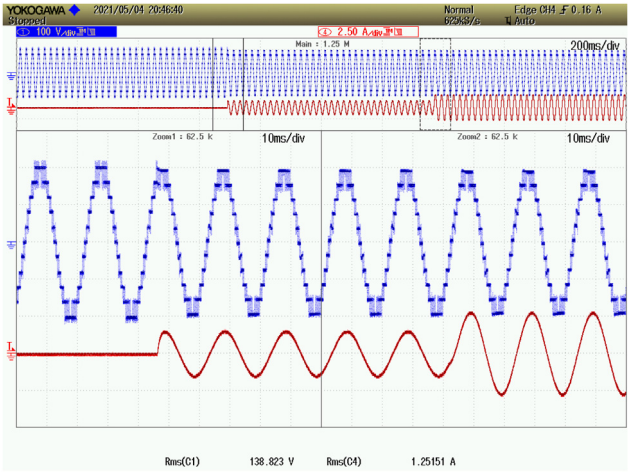

Fig. 14. SPWM of the same inverter.

in a quarter period is considered, the cell '1' is turned on and off with angles as α_1 ↑, α_2 ↓ and α_3 ↑. The cell '1' output voltages have three voltage levels as $+V_{dc}$, 0 and $-V_{dc}$. similarly second and third cells switching logics is designed. The logic for generation of gate pulse of cell '1' with three switching angles is created by comparing the sine values of switching angles with a 50 Hz sine modulation reference signal as shown in Fig. 15. Similarly the gate pulses for cell '2' and '3' are generated. The output voltage, current waveform and harmonics profile at $M = 0.80$, $M = 0.85$ for the cases given in Table 4 ($'I'$ and $'II'$) have been shown in Fig. 16. It is evident from the harmonics profile that the targeted harmonics for minimization are absent in the output voltage waveform. The voltage and current waveforms along-with harmonics profile for multiple switching of RL load is shown in Fig. 17.

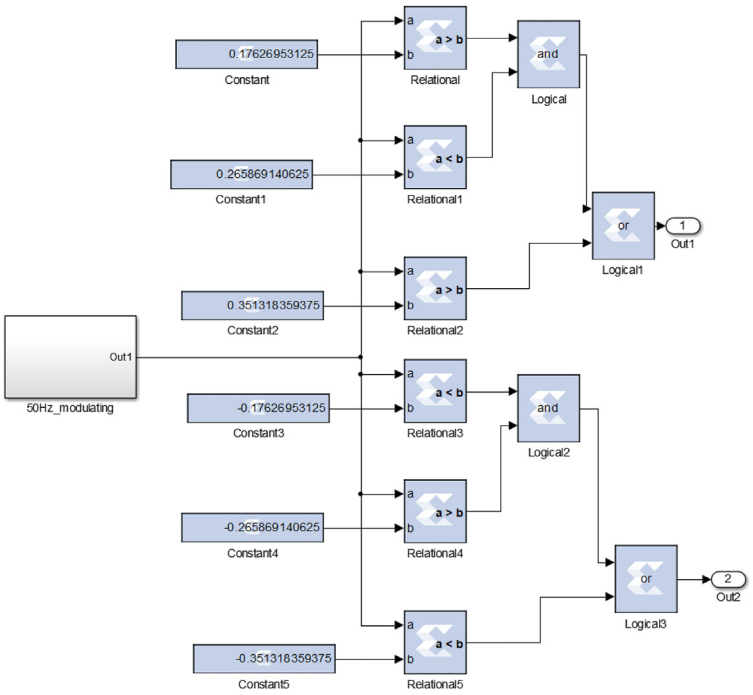

Fig. 15. Multiple switching gate pulse generation for cell '1'.

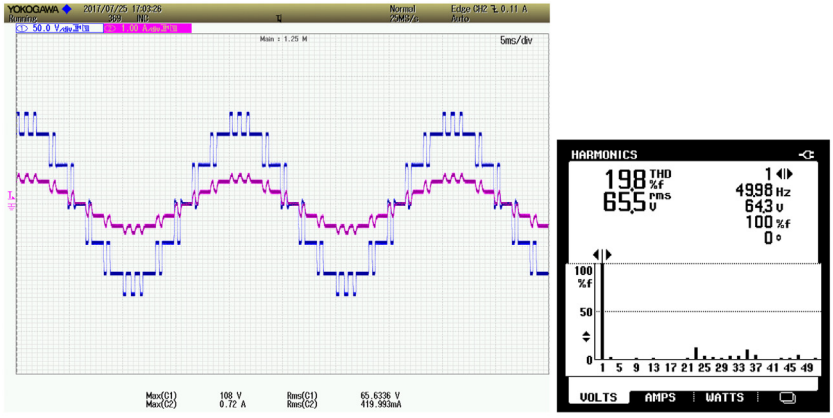

(a) Output voltage and currents (b) Harmonics profile

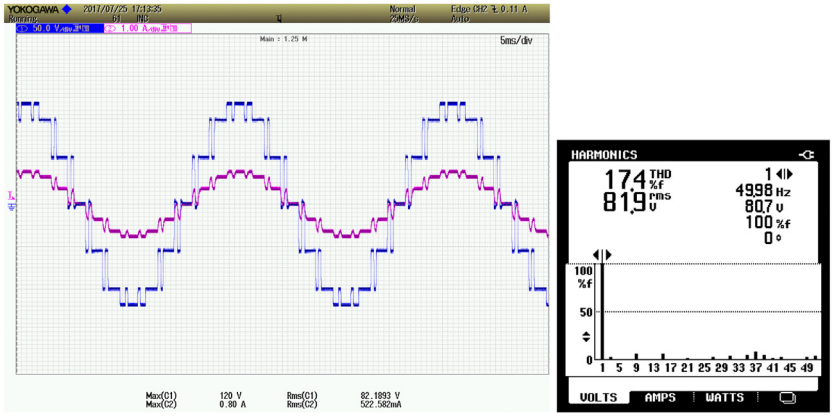

(c) Output voltage and currents (d) Harmonics profile

Fig. 16. Multiple pulse seven level asymmetric waveforms.

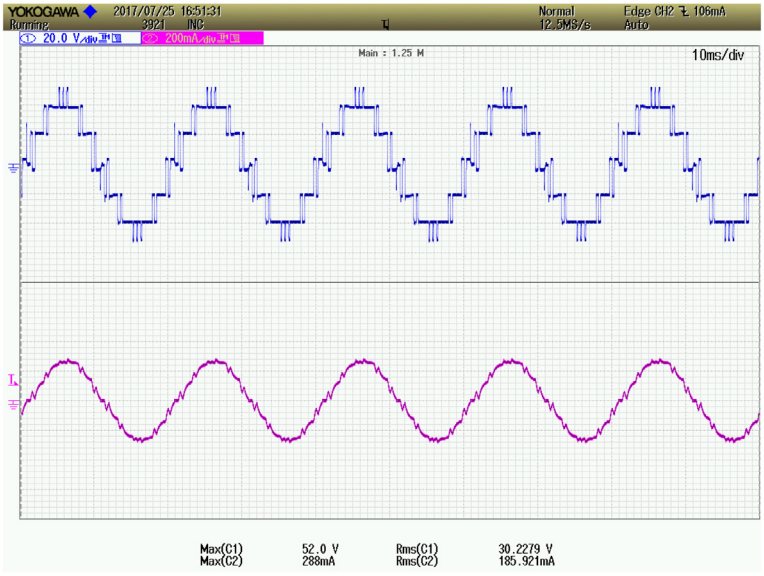

(a) Output voltage and current

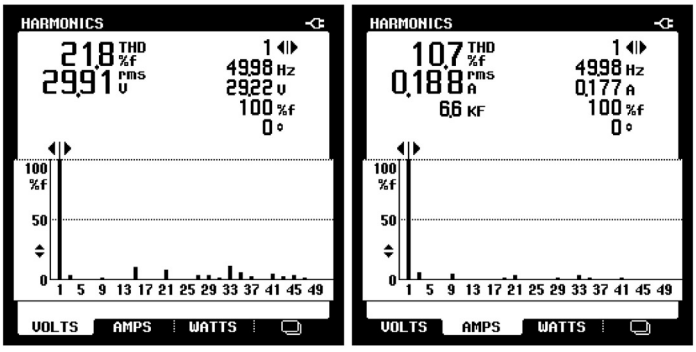

(b) Volage harmonics (c) Current harmonics

Fig. 17. Voltage waveform and harmonics profile at RL load.

6. Conclusion

In this paper a novel invasive weed algorithm is proposed for obtaining the switching angles in order to minimize the selected lower order harmonics from the output waveform. The proposed algorithm have been successfully implemented for fundamental to multiple of fundamental switching frequency for symmetrical and asymmetrical multilevel inverters. The large size transcendental equations in several variables (switching angles and dc-voltage) have been solved by the proposed technique, where other conventional methods fails. The performance of IWO method have been compared with other optimization methods such as GA, PSO, DE, ACO, CCA, ABC and TL. The IWO shows faster convergence and better accuracy compared to other optimization techniques. The experimental results have been obtained on 1 kW prototype created with SIC-MOSFET FDP19N40 of 1200 V, 40 A ratings and gate pulses are generated by Virtex-5 FPGA digital controller. The symmetrical and asymmetrical output waveforms for fundamental and multiple switching on R and RL load with step change validates the accuracy of the computed switching angles. The harmonics profile shows that the targeted harmonics have been minimized. The harmonics minimization technique are extremely useful in medium voltage and high power applications of voltage source converters such as in variable speed drives, static compensator, grid integration of solar PV systems with minimum filtering requirements etc.

CRediT authorship contribution statement

Salman Ahmad: Preparing, Problem formulation, Writing, Conducting experiments. **Atif Iqbal:** Preparing, Problem formulation, Writing, Conducting experiments. **Imtiaz Ashraf:** Preparing, Problem formulation, Writing, Conducting experiments. **Mohammad Meraj:** Preparing, Problem formulation, Writing, Conducting experiments.

Declaration of competing interest

The authors declare that they have no known competing financial interests or personal relationships that could have appeared to influence the work reported in this paper.

Acknowledgement

This publication was made possible by NPRP grant #[13S-0108-20008] from the Qatar National Research Fund (A member of Qatar Foundation). The statements made herein are solely the responsibility of the authors. The APC of the paper is funded by the Qatar National Library, Doha, Qatar.

```
%% Problem Definition
M=0; k=1;
CostFunction = @(x) ObLatest35(x);
nVar = 5;  VarSize = [1 nVar];  VarMin = 0;   VarMax = pi()/2;
 %% IWO Parameters
MaxIt = 500;    nPop0 = 10;  nPop = 25;  Smin = 0;   Smax = 5;   Exponent = 2;
sigma_initial = 0.5;  sigma_final = 0.001;
%% Initialization
while (M<1)
empty_plant.Position = []; empty_plant.Cost = []; pop = repmat(empty_plant, nPop0,
1);
for i = 1:numel(pop)
      pop(i).Position = unifrnd(VarMin, VarMax, VarSize);
   % Evaluation
   pop(i).Cost = CostFunction(pop(i).Position); end
 % Initialize Best Cost History
BestCosts = zeros(MaxIt, 1);
 %% IWO Main Loop
 for it = 1:MaxIt
      % Update Standard Deviation
   sigma = ((MaxIt - it)/(MaxIt - 1))^Exponent * (sigma_initial - sigma_final) +
sigma_final;
   % Get Best and Worst Cost Values
   Costs = [pop.Cost]; BestCost = min(Costs); WorstCost = max(Costs);
   % Initialize Offsprings Population
   newpop = [];
   % Reproduction
   for i = 1:numel(pop)
      ratio = (pop(i).Cost - WorstCost)/(BestCost - WorstCost); S = floor(Smin + (Smax -
Smin)*ratio);
      for j = 1:S
         % Initialize Offspring
         newsol = empty_plant;
         % Generate Random Location
         newsol.Position = pop(i).Position + sigma * randn(VarSize);
         % Apply Lower/Upper Bounds
         newsol.Position = max(newsol.Position, VarMin);
         newsol.Position = min(newsol.Position, VarMax);
         % Evaluate Offsring
         newsol.Cost = CostFunction(newsol.Position);
         % Add Offpsring to the Population
         newpop = [newpop newsol]; end end
      % Merge Populations
   pop = [pop newpop];
   % Sort Population
   [~, SortOrder]=sort([pop.Cost]); pop = pop(SortOrder);
   % Competitive Exclusion (Delete Extra Members)
   if numel(pop)>nPop
      pop = pop(1:nPop);
   end
   % Store Best Solution Ever Found
   BestSol = pop(1);
   % Store Best Cost History
   BestCosts(it) = BestSol.Cost;
   % Display Iteration Information
   disp(['Iteration ' num2str(it) ': Best Cost = ' num2str(BestCosts(it))]); end
 A=sort(BestSol.Position);
G=(BestSol.Cost);
if G<=0.00001;
            R(k,:)=[M A G it];
        k=k+1;   end
 M=M+0.0001;
end
```

Appendix

See the listing given.

References

Ahmad, S., Iqbal, A., Ali, M., Rahman, K., Ahmed, A.S., 2021. A fast convergent homotopy perturbation method for solving selective harmonics elimination PWM problem in multi level inverter. IEEE Access 9, 113040–113051.

Ahmad, S., Meraj, M., Iqbal, A., Ashraf, I., 2019. Selective harmonics elimination in multilevel inverter by a derivative-free iterative method under varying voltage condition. ISA Trans. 92, 241–256.

Ahmed, M., Aziz, T., et al., 2021. An approach of incorporating harmonic mitigation units in an industrial distribution network with renewable penetration. Energy Rep. 7, 6273–6291.

Ahmed, M., Orabi, M., Ghoneim, S.S., Al-Harthi, M.M., Salem, F.A., Alamri, B., Mekhilef, S., 2019. General mathematical solution for selective harmonic

elimination. IEEE J. Emerg. Sel. Top. Power Electron. 8 (4), 4440–4456.
Ali, M., Din, Z., Solomin, E., Cheema, K.M., Milyani, A.H., Che, Z., 2021. Open switch fault diagnosis of cascade H-bridge multi-level inverter in distributed power generators by machine learning algorithms. Energy Rep. 7, 8929–8942.
Bagdadee, A.H., Khan, M.Y.A., Ding, H., Cao, J., Zhang, L., Ding, Y., 2020. Implement industrial super-dynamic voltage recovery equipment for power quality improvement in the industrial sector. Energy Rep. 6, 1167–1175.
Balasubramonian, M., Rajamani, V., 2014. Design and real-time implementation of SHEPWM in single-phase inverter using generalized hopfield neural network. IEEE Trans. Ind. Electron. 61 (11), 6327–6336.
Chen, D., Xiao, L., Yan, W., Li, Y., Guo, Y., 2021. A harmonics detection method based on triangle orthogonal principle for shunt active power filter. Energy Rep..
Chen, H., Zhao, H., 2016. Review on pulse-width modulation strategies for common-mode voltage reduction in three-phase voltage-source inverters. IET Power Electron. 9 (14), 2611–2620.
Chiasson, J., Tolbert, L.M., McKenzie, K., Du, Z., 2003. A complete solution to the harmonic elimination problem. In: Eighteenth Annual IEEE Applied Power Electronics Conference and Exposition, 2003. APEC'03, Vol. 1. IEEE, pp. 596–602.
Colak, I., Kabalci, E., Bayindir, R., 2011. Review of multilevel voltage source inverter topologies and control schemes. Energy Convers. Manage. 52 (2), 1114–1128.
Dahidah, M.S., Konstantinou, G., Agelidis, V.G., 2014. A review of multilevel selective harmonic elimination PWM: formulations, solving algorithms, implementation and applications. IEEE Trans. Power Electron. 30 (8), 4091–4106.
Edpuganti, A., Rathore, A.K., 2015. A survey of low switching frequency modulation techniques for medium-voltage multilevel converters. IEEE Trans. Ind. Appl. 51 (5), 4212–4228.
Eguchi, K., Shibata, A., Do, W., Harada, Y., 2020. An inductor-less step-up/step-down multilevel inverter with a single input source. Energy Rep. 6, 146–152.
Enjeti, P.N., Ziogas, P.D., Lindsay, J.F., 1988. Programmed PWM techniques to eliminate harmonics-a critical evaluation. In: Conference Record of the 1988 IEEE Industry Applications Society Annual Meeting. IEEE, pp. 418–430.
Etesami, M., Farokhnia, N., Fathi, S.H., 2015. Colonial competitive algorithm development toward harmonic minimization in multilevel inverters. IEEE Trans. Ind. Inform. 11 (2), 459–466.
Gupta, K.K., Bhatnagar, P., 2017. Multilevel Inverters: Conventional And Emerging Topologies And Their Control. Academic Press.
Gupta, K.K., Ranjan, A., Bhatnagar, P., Sahu, L.K., Jain, S., 2015. Multilevel inverter topologies with reduced device count: A review. IEEE Trans. Power Electron. 31 (1), 135–151.
Hagh, M.T., Taghizadeh, H., Razi, K., 2009. Harmonic minimization in multilevel inverters using modified species-based particle swarm optimization. IEEE Trans. Power Electron. 24 (10), 2259–2267.
Haghdar, K., 2019. Optimal DC source influence on selective harmonic elimination in multilevel inverters using teaching–learning-based optimization. IEEE Trans. Ind. Electron. 67 (2), 942–949.
Holmes, D.G., Lipo, T.A., 2003. Pulse Width Modulation For Power Converters: Principles And Practice, Vol. 18. John Wiley & Sons.
Janabi, A., Wang, B., Czarkowski, D., 2019. Generalized chudnovsky algorithm for real-time PWM selective harmonic elimination/modulation: two-level VSI example. IEEE Trans. Power Electron. 35 (5), 5437–5446.
Janardhan, K., Mittal, A., Ojha, A., 2020. Performance investigation of stand-alone solar photovoltaic system with single phase micro multilevel inverter. Energy Rep. 6, 2044–2055.
Kavousi, A., Vahidi, B., Salehi, R., Bakhshizadeh, M.K., Farokhnia, N., Fathi, S.H., 2011. Application of the bee algorithm for selective harmonic elimination strategy in multilevel inverters. IEEE Trans. Power Electron. 27 (4), 1689–1696.
Kouro, S., Malinowski, M., Gopakumar, K., Pou, J., Franquelo, L.G., Wu, B., Rodriguez, J., Pérez, M.A., Leon, J.I., 2010. Recent advances and industrial applications of multilevel converters. IEEE Trans. Ind. Electron. 57 (8), 2553–2580.
Kularbphettong, K., Boonseng, C., 2020. HPFs filtering solutions for reduced the harmonic current generated by SMPS and ac drive systems. Energy Rep. 6, 648–658.
Kumari, M., Ali, M., Ahmad, S., Ashraf, I., Azeem, A., Tariq, M., Arif, M.S.B., Iqbal, A., 2019. Genetic algorithm based SHE-PWM for 1-øand 3-øvoltage source inverters. In: 2019 International Conference on Power Electronics, Control and Automation. ICPECA, IEEE, pp. 1–6.
Kundu, S., Bhowmick, S., Banerjee, S., 2019. Improvement of power utilisation capability for a three-phase seven-level CHB inverter using an improved selective harmonic elimination–PWM scheme by sharing a desired proportion of power among the H-bridge cells. IET Power Electron. 12 (12), 3242–3253.
Kundu, S., Burman, A.D., Giri, S.K., Mukherjee, S., Banerjee, S., 2017. Comparative study between different optimisation techniques for finding precise switching angle for SHE-PWM of three-phase seven-level cascaded H-bridge inverter. IET Power Electron. 11 (3), 600–609.
Levi, E., Bojoi, R., Profumo, F., Toliyat, H., Williamson, S., 2007. Multiphase induction motor drives–a technology status review. IET Electr. Power Appl. 1 (4), 489–516.
Maia, H.Z., Mateus, T.H., Ozpineci, B., Tolbert, L.M., Pinto, J.a.O., et al., 2012. Adaptive selective harmonic minimization based on ANNs for cascade multilevel inverters with varying DC sources. IEEE Trans. Ind. Electron. 60 (5), 1955–1962.
Mehrabian, A.R., Lucas, C., 2006. A novel numerical optimization algorithm inspired from weed colonization. Ecol. Inform. 1 (4), 355–366.
Memon, M.A., Mekhilef, S., Mubin, M., Aamir, M., 2018. Selective harmonic elimination in inverters using bio-inspired intelligent algorithms for renewable energy conversion applications: A review. Renew. Sustain. Energy Rev. 82, 2235–2253.
Memon, M.A., Siddique, M.D., Saad, M., Mubin, M., 2021. Asynchronous particle swarm optimization-genetic algorithm (APSO-GA) based selective harmonic elimination in a cascaded H-bridge multilevel inverter. IEEE Trans. Ind. Electron..
Misaghi, M., Yaghoobi, M., 2019. Improved invasive weed optimization algorithm (IWO) based on chaos theory for optimal design of PID controller. J. Comput. Des. Eng. 6 (3), 284–295.
Panda, K.P., Bana, P.R., Panda, G., 2020. FPA optimized selective harmonic elimination in symmetric–asymmetric reduced switch cascaded multilevel inverter. IEEE Trans. Ind. Appl. 56 (3), 2862–2870.
Panda, K.P., Panda, G., 2018. Application of swarm optimisation-based modified algorithm for selective harmonic elimination in reduced switch count multilevel inverter. IET Power Electron. 11 (8), 1472–1482.
Patel, H.S., Hoft, R.G., 1973. Generalized techniques of harmonic elimination and voltage control in thyristor inverters: Part I–Harmonic elimination. IEEE Trans. Ind. Appl. (3), 310–317.
Plangklang, B., Thanomsat, N., Phuksamak, T., 2016. A verification analysis of power quality and energy yield of a large scale PV rooftop. Energy Rep. 2, 1–7.
Rao, S.S., 2019. Engineering Optimization: Theory and Practice. John Wiley & Sons.
Roberge, V., Tarbouchi, M., Labonté, G., 2015. Parallel algorithm on graphics processing unit for harmonic minimization in multilevel inverters. IEEE Trans. Ind. Inform. 11 (3), 700–707.
Salam, Z., Majed, A., Amjad, A.M., 2015. Design and implementation of 15-level cascaded multi-level voltage source inverter with harmonics elimination pulse-width modulation using differential evolution method. IET Power Electron. 8 (9), 1740–1748.
Salam, Z., Yee, S.S., Saleem, Y., 2013. On the improved computational speed and convergence of the Newton raphson iteration method for selective harmonics elimination PWM applied to cascaded multilevel inverter with equal and non-equal DC sources. COMPEL - Int. J. Comput. Math. Electr. Electron. Eng..
Sundareswaran, K., Jayant, K., Shanavas, T., 2007. Inverter harmonic elimination through a colony of continuously exploring ants. IEEE Trans. Ind. Electron. 54 (5), 2558–2565.
Swift, F., Kamberis, A., 1993. A new Walsh domain technique of harmonic elimination and voltage control in pulse-width modulated inverters. IEEE Trans. Power Electron. 8 (2), 170–185.
Tashakor, N., Li, Z., Goetz, S.M., 2020. A generic scheduling algorithm for low-frequency switching in modular multilevel converters with parallel functionality. IEEE Trans. Power Electron. 36 (3), 2852–2863.
Tolbert, L.M., Cao, Y., Ozpineci, B., et al., 2011. Real-time selective harmonic minimization for multilevel inverters connected to solar panels using artificial neural network angle generation. IEEE Trans. Ind. Appl. 47 (5), 2117–2124.
Venkataramanaiah, J., Suresh, Y., Panda, A.K., 2017. A review on symmetric, asymmetric, hybrid and single DC sources based multilevel inverter topologies. Renew. Sustain. Energy Rev. 76, 788–812.
Wu, M., Li, Y.W., Konstantinou, G., 2020. A comprehensive review of capacitor voltage balancing strategies for multilevel converters under selective harmonic elimination PWM. IEEE Trans. Power Electron. 36 (3), 2748–2767.
Wu, B., Narimani, M., 2017. High-Power Converters And AC Drives. John Wiley & Sons.
Yang, K., Zhang, Q., Yuan, R., Yu, W., Yuan, J., Wang, J., 2015. Selective harmonic elimination with Groebner bases and symmetric polynomials. IEEE Trans. Power Electron. 31 (4), 2742–2752.